Overview of the Lake Michigan Ozone Study 2017

Charles O. Stanier,[a] R. Bradley Pierce,[b] Maryam Abdi-Oskouei,[a,c] Zachariah E. Adelman,[d] Jay Al-Saadi,[e] Hariprasad D. Alwe,[f] Timothy H. Bertram,[g] Gregory R. Carmichael,[a] Megan B. Christiansen,[a] Patricia A. Cleary,[h] Alan C. Czarnetzki,[i] Angela F. Dickens,[d,j] Marta A. Fuoco,[k] Dagen D. Hughes,[a] Joseph P. Hupy,[l] Scott J. Janz,[m] Laura M. Judd,[e] Donna Kenski,[d] Matthew G. Kowalewski,[m] Russell W. Long,[o] Dylan B. Millet,[f] Gordon Novak,[g] Behrooz Roozitalab,[a] Stephanie L. Shaw,[n] Elizabeth A. Stone,[a] James Szykman,[o] Lukas Valin,[o] Michael Vermeuel,[g] Timothy J. Wagner,[b] Andrew R. Whitehill,[o] David J. Williams[o]

[a] *University of Iowa, Iowa City, IA*

[b] *Space Science and Engineering Center, University of Wisconsin, Madison, WI*

[c] *now at University Corporation for Atmospheric Research (UCAR), Boulder, CO*

[d] *Lake Michigan Air Directors Consortium (LADCO), Chicago, IL*

[e] *NASA Langley Research Center, Hampton, VA*

[f] *University of Minnesota, Saint Paul, MN*

[g] *University of Wisconsin, Madison, WI*

[h] *University of Wisconsin, Eau Claire, WI*

[i] *University of Northern Iowa, Cedar Falls, IA*

[j] *Wisconsin Department of Natural Resources, Madison, WI*

[k] *U.S. EPA Region 5, Chicago, IL*

[l] *Purdue University, West Lafayette, IN*

[m] *NASA Goddard Space Flight Center, Greenbelt, MD*

[n] *Electric Power Research Institute, Palo Alto, CA*

[o] *Center for Environmental Measurement and Modeling, United States Environmental Protection Agency*

Corresponding author: Charles O. Stanier, charles-stanier@uiowa.edu

Early Online Release: This preliminary version has been accepted for publication in *Bulletin of the American Meteorological Society*, may be fully cited, and has been assigned DOI 10.1175/BAMS-D-20-0061.1. The final typeset copyedited article will replace the EOR at the above DOI when it is published.

ABSTRACT

The Lake Michigan Ozone Study 2017 (LMOS 2017) was a collaborative multi-agency field study targeting ozone chemistry, meteorology, and air quality observations in the southern Lake Michigan area. The primary objective of LMOS 2017 was to provide measurements to improve air quality modeling of the complex meteorological and chemical environment in the region. LMOS 2017 science questions included spatiotemporal assessment of nitrogen oxides (NO_x = NO + NO_2) and volatile organic compounds (VOC) emission sources and their influence on ozone episodes, the role of lake breezes, contribution of new remote sensing tools such as GeoTASO, Pandora, and TEMPO to air quality management, and evaluation of photochemical grid models. The observing strategy included GeoTASO on board the NASA UC-12 capturing NO_2 and formaldehyde columns, an in situ profiling aircraft, two ground-based coastal enhanced monitoring locations, continuous NO_2 columns from coastal Pandora instruments, and an instrumented research vessel. Local photochemical ozone production was observed on 2 June, 9–12 June, and 14–16 June, providing insights on the processes relevant to state and federal air quality management. The LMOS 2017 aircraft mapped significant spatial and temporal variation of NO_2 emissions as well as polluted layers with rapid ozone formation occurring in a shallow layer near the Lake Michigan surface. Meteorological characteristics of the lake breeze were observed in detail and measurements of ozone, NO_x, nitric acid, hydrogen peroxide, VOC, oxygenated VOC (OVOC), and fine particulate matter ($PM_{2.5}$) composition were conducted. This article summarizes the study design, directs readers to the campaign data repository, and presents a summary of findings.

CAPSULE

The Lake Michigan Ozone Study (LMOS 2017) was an enhanced observational study aimed at better understanding ozone formation and transport over Lake Michigan and surrounding coastal communities.

Introduction

Urban-influenced coastal environments are an air quality management challenge because of complex wind patterns, shallow stable marine boundary layers, and the interaction of these meteorological features with ozone precursor (reactive nitrogen and volatile organic compound, VOC) emissions. Many of the counties in the eastern U.S. where ozone concentrations exceed the 2015 ozone National Ambient Air Quality Standards (NAAQS) of 70 ppb are along coastlines (USEPA, 2015). Studies such as the Lake Michigan Air Quality Study 1991 (Dye et al., 1995), Lake Michigan Air Directors Consortium (LADCO) Aircraft Project (LAP 1994–2003) (Foley et al., 2011), Border Air Quality and Meteorology Study (BAQS-Met) (Makar et al., 2010), Ozone Water- Land Environmental Transition Study (OWLETS) (Sullivan et al., 2019), Long Island Sound Tropospheric Ozone Study (LISTOS) (Miller, 2018; Zhang et al., 2020), and the Baltimore-Washington and Houston legs of DISCOVER-AQ (Mazzuca et al., 2016) have sought to improve understanding of coastal air quality and meteorological interactions. The Lake Michigan Ozone Study 2017 (LMOS 2017), a recent collaborative, multi- agency field study targeting ozone chemistry, meteorology, and related air quality observations along the Wisconsin- Illinois Lake Michigan shoreline, built on these previous studies, and adapted new observing platforms and modeling capabilities. In this manuscript, we give an overview of the rationale for LMOS 2017 along with its study design and some principal results.

Around Lake Michigan, both rural and urban monitoring locations have persistently recorded high ozone concentrations that continue to exceed the ozone NAAQS as of 31 January 2021 (https://www.epa.gov/green-book). 1-hour and 8-hour maximum concentrations have decreased substantially over the past three decades in conjunction with large decreases in emissions of

ozone precursors. In EPA Region 5 (consisting of Illinois, Indiana, Michigan, Minnesota, Ohio, Wisconsin) anthropogenic nitrogen oxides (NO_x=NO+NO_2) and VOC emissions dropped 65% and 52%, respectively (Adelman, 2020) between 1997 and 2017. However, the ozone NAAQS was lowered to 75 ppb in 2008 and to 70 ppb in 2015 in response to health-focused science that showed further reductions of ozone were necessary for human health protection (USEPA, 2006, 2103). As a result, current and future additional controls on NO_x and VOC emissions will likely be required in the region to achieve attainment status.

Ozone concentrations for the 3-year period from 2014 to 2016 (Figure 1) show some of the locations exceeding the NAAQS (70 ppb) which motivated the field campaign. As Figure 1 shows, the highest ozone concentrations in the Lake Michigan region have been found along the lakefront, consistent with elevated ozone concentrations over Lake Michigan (Dye et al., 1995; Foley et al., 2011; Cleary et al., 2015). Lake Michigan's air quality episodes often occur when weak synoptic southerly winds, common during fair weather periods, interact with lake breezes (Lyons and Olsson, 1973; Lennartson and Schwartz, 2002). For the western coast of Lake Michigan, ozone exceedances are most frequent from late May to early July (Good, 2017), and during this time period, the lake water temperatures (8–17 °C) are substantially colder than the surrounding land (Laird et al., 2001). Lake breeze flows commence in late morning, and are sometimes accompanied by offshore nighttime flows (driven by land radiative cooling) that lead to warmer temperatures over the lake relative to land. Under these conditions, emissions can be trapped when they are drawn out over the lake during night or early morning. This is followed by photochemical ozone production confined in a shallow lake inversion layer. Finally, processed plumes that have undergone substantial oxidation can return onshore with elevated ozone levels during midday and afternoon.

Dye et al. (1995) clearly showed the role of the shallow stable conduction layer over the lake during ozone episodes. The limited vertical mixing in this layer coupled with stability and slow deposition – due to lack of surface roughness – creates an excellent reactor for ozone production and accumulation. In classic Lake Michigan ozone pollution events, synoptic winds from the south and southwest push pollution plumes from the Chicago and Milwaukee metropolitan areas out over the lake, and late morning or afternoon lake breezes transport them back to the coastline. Emission sources outside the major population centers must also be considered against this conduction layer enhancement.

To best support ongoing air quality management decisions aimed at lowering ozone in the remaining non-attainment areas, LMOS 2017 was conceived to gather new observations of ozone, ozone precursors, and meteorology. Such measurements were required to evaluate air quality and meteorology models, which are run at increasingly high spatial resolutions with a very wide variety of choices for physics, chemistry, data inputs, and data assimilation options. These diverse characteristics make configuration selection challenging for the best forecasting and regulatory modeling of ozone episodes. Air quality models are also dependent on emission inventories that have large potential errors due to rapid changes in electrical generation and mobile sectors coupled with uncertainties in emission and speciation for VOC.

The measurement strategy for LMOS 2017 sought to take advantage of recent observational advances including increasingly fast and sensitive in-situ chemical measurements, active and passive ground based remote sensing, and new airborne remote sensing capabilities (see sidebar Preparing for New Air Quality Monitoring Capabilities). Furthermore, the LMOS team aimed to use the study as an initial assessment of how improved satellite-based measurements of meteorology and air quality might be applied to ozone pollution management in airsheds such as

Lake Michigan, which have heterogeneous land use and emissions coupled with complex meteorological transport. LMOS 2017 was also an example of the increasingly common grassroots field study structure, where early commitments for resources (e.g., NOAA satellite validation, NASA flight hours, EPA mobile lab, state and local personnel, equipment, and site access) seeded further investments (NSF, industry) around a coherent set of science objectives.

The scientific questions of the LMOS 2017 field campaign were the following:

1. What is the relative contribution of inter- and intra-state NO_x and VOC emission sources on ozone production rates along Lake Michigan?
2. To what extent do lake breeze circulations affect ozone production?
3. How far inland does ozone-rich air penetrate during ozone events?
4. What is the spatio-temporal distribution of ozone and its precursors over Lake Michigan?
5. How can remote sensing products (e.g., measurements of nitrogen dioxide, NO_2, and formaldehyde) be used to constrain ozone predictions?
6. How well do regional models capture ozone production chemistry as assessed through evaluation of critical observation-based indicators (e.g., formaldehyde:NO_x ratio)?

In the remainder of the article, we first present the study design, measurement locations, and observation platforms. We then present a high-level overview of the air quality and meteorological conditions observed during LMOS 2017, and discuss multi-model underprediction of peak ozone in both forecast and post-analysis configurations. We conclude with a summary of study findings to date and invitation for the community to access the LMOS

2017 data at the NASA campaign repository. LMOS 2017 post-analysis work has made progress on all of the science questions, but additional work remains. We invite the scientific community to utilize the unique set of measurements collected during LMOS 2017 to continue to address these science questions in collaboration with university, federal, and state partners.

Study Design

LMOS 2017 focused on ozone precursor emissions, ozone chemistry, and associated meteorology over the southwestern portion of Lake Michigan and along the western shore of Lake Michigan from Chicago, IL, to Sheboygan, WI. As shown in Figure 2, the measurement strategy incorporated a combination of ground sites, aircraft and ship sampling, and mobile vehicles. The strategy relied on (1) ground-based sites close to the lake shore to capture onshore flows of oxidatively processed ozone-rich air, and (2) airborne platforms for large-scale mapping and vertical profiling. Supported by preliminary modeling using the Weather Research and Forecasting model with Chemistry (WRF-Chem) model, and the locations of the highest ozone design values, two ground-based enhanced monitoring (EM) sites were used (design values are an EPA air quality evaluation based on the most recent 3 years of observations; lower values represent cleaner conditions; see Fig. 1 caption for more detail). A southerly ground-based EM site was established at Zion, IL (67 km north of Chicago), to intercept relatively fresh urban plumes with elevated precursor concentrations. A more northerly EM site was established at Sheboygan, WI (211 km north of Chicago), to intercept plumes at a greater distance from sources after more extensive oxidative aging. Contrasting ground sites of these types are critical for testing photochemical grid models (PGM) such as WRF-Chem, the Community Multi-scale

Air Quality (CMAQ) model, and the Comprehensive Air Quality Model with Extensions (CAMx).

Along with the EM sites, two aircraft platforms were fundamental to the LMOS 2017 observing strategy. The NASA LaRC UC-12 flew 21 research flights during LMOS 2017. On board the UC-12 were the Geostationary Trace gas and Aerosol Sensor Optimization (GeoTASO, Leitch et al. 2014) instrument from which vertical columns of NO_2 and formaldehyde were retrieved, and the Airborne Hyper Angular Rainbow Polarimeter (AirHARP, McBride et al. 2020), which measured physical and optical properties of aerosols and clouds. A light aircraft (Scientific Aviation, SA, Mooney Ovation 2, N334FL) flew 22 research flights, measuring in situ NO_2, ozone, carbon dioxide, methane, and meteorological parameters (temperature, pressure, horizontal wind speed and direction, and water vapor mixing ratio).

Table 1 lists the major measurement platforms and their locations or areas of operation for LMOS 2017. Brief descriptions of each platform or site's capabilities are given below. A supplemental information table contains a full list of measurement platforms and instruments, and measurements are publicly available at the NASA LaRC data repository (https://www-air.larc.nasa.gov/cgi-bin/ArcView/lmos). Many of the instruments and observations are discussed in previous LMOS team publications such as the LADCO Synthesis report (Abdi-Oskouei et al., 2019) as well other LMOS 2017 publications (Judd et al., 2019; Vermeuel et al., 2019; Abdi-Oskouei et al., 2020; Doak et al., 2021; Hughes et al., 2021).

Ground-based enhanced monitoring sites.

Accepted for publication in *Bulletin of the American Meteorological Society*. DOI 10.1175/BAMS-D-20-0061.1.

186 The EM sites were chosen due to their proximity to the coast and high ozone design values
187 that would benefit from more accurate emissions, chemistry, and transport modeling for design
188 of attainment strategies.

189 The Zion EM site was located 1 km from the shoreline at Illinois Beach State Park. This site
190 hosts an Illinois EPA State and Local Air Monitoring Station (SLAMS) that provides data to the
191 U.S. Air Quality System (AQS). The Illinois Beach State Park station is site 17-097-1007
192 (42.468 N, 87.810 W). The Zion site also benefits from proximity to the Chiwaukee, WI SLAMS
193 station, which had one of the highest 2014–2016 design values in the study domain (77 ppb). At
194 Zion, IL, a dataset of continuous wind, temperature, and water vapor vertical profile was
195 recorded using sodar and microwave radiometer (MR) instruments. These instruments captured
196 thermal and wind characteristics of lake breeze penetration with high vertical and temporal
197 resolution. Continuous or semi-continuous measurements of ozone, NO_x, nitric acid, hydrogen
198 peroxide, and many VOC and oxygenated volatile organic compounds (OVOC) were conducted.
199 These measurements, in conjunction with detailed Lagrangian photochemical model
200 calculations, have been used to assess the relative importance of NO_x and VOC emissions in
201 determining ozone production at the Zion EM site (Vermeuel et al. 2019). Finally,
202 comprehensive chemical and physical aerosol characterization was conducted to enable source
203 apportionment and study of oxidative chemistry (Hughes et al. 2021).

204 The Sheboygan EM site (43.745 N, 87.709 W) was located at the Spaceport science
205 education facility near the harbor in Sheboygan; the site was 250 m from the shoreline and 8.75
206 km north of the WDNR Sheboygan Kohler Andrae (KA) monitoring station. The Sheboygan KA
207 monitor had the highest 2014–2016 ozone design value in the study domain (79 ppb, see Figure

1). In this document, the Sheboygan site refers to the temporary campaign measurement site near the Sheboygan harbor; Sheboygan KA refers to the long-term monitoring site at Kohler Andrae.

The UW-Madison Space Science and Engineering Center (SSEC) Portable Atmospheric Research Center (SPARC, Wagner et al., 2019) was deployed at the Sheboygan site. It housed the Atmospheric Emitted Radiance Interferometer (AERI, Knuteson et al., 2004), Doppler lidar, and high spectral resolution (HSRL) aerosol lidar instruments to provide continuous profiles of temperature, water vapor, winds, and aerosol backscatter. This combination of instruments enabled detailed observation of many aspects of the lake breeze. In situ chemical measurements at the Sheboygan site included ozone, NO_x, formaldehyde, and NO_x plus its reaction products (NO_y) at 1-minute and finer time resolution. An experimental network of four low-cost ozone monitors (POM, 2B Technologies) was deployed over a 6-km^2 area of Sheboygan, WI, to measure differences in concentrations with respect to distance from the lake.

Air pollution sources, both at ground-level and from elevated stacks, exist throughout the study domain. For example, both EM sites had nearby Electric Generation Units (EGUs). The Zion site was located 11 km southeast of the Pleasant Prairie Power Plant while the Sheboygan site was located 3.35 km north of the Edgewater Generating Station. One of the study goals was to use the suite of meteorological and chemical measurements to characterize the impact of localized emissions during ozone episodes and other time periods. High resolution air quality modeling studies guided by the LMOS measurements, are currently underway to explore the impact of these localized emissions on ozone production at the Sheboygan and Zion EM sites.

Other ground-based remote sensing.

In addition to the meteorological sensors at the EM sites described above, the U.S. Environmental Protection Agency deployed remote sensing instruments for mixed layer height, cloud layer height, column NO_2, and column ozone (Vaisala CL51 ceilometers and UV/visible Pandora spectrometers). The ceilometers were installed at Grafton, Milwaukee, and Zion. The Pandora spectrometers were installed at the Sheboygan site, as well as WDNR monitoring sites in Grafton, Milwaukee, and Illinois EPA monitoring sites in Zion, and Schiller Park (Chicago). Data on mixed layer height, ozone column amounts, and NO_2 column amounts are being included in ongoing analyses including comparison to models, comparison to aircraft in situ profiles, and comparison to other remotely sensed atmospheric composition products.

Aircraft measurements.

Primary flight objectives were to (1) conduct regional-scale coastal surveys along the western shore of Lake Michigan during ozone exceedance events, (2) conduct local flights over Chicago, IL, and Milwaukee, WI, to characterize the NO_2 emissions, and (3) conduct local flights in the vicinity of Sheboygan, WI, and Zion, IL, to characterize coastal gradients in air pollutants and meteorological fields.

The NASA Langley Research Center UC-12 aircraft carrying GeoTASO focused on remote measurements of NO_2 and formaldehyde using raster pattern flight plans to obtain maps of NO_2 column abundances. In situ trace gas and meteorological measurements were made using instruments onboard a Mooney Aircraft operated by Scientific Aviation. Flying at 28,000 ft, the UC-12 was able to perform remote sensing over the entire study domain, including over airport flight restriction zones which can reach up to 10,000 ft. Scientific Aviation, on the other hand, flew low-level transects to sample the marine boundary layer along with in situ spirals to measure vertical profiles at selected waypoints. On most of the deployment days, the two aircraft

252 flew over the same area at the same time to provide the best overlap between the two types of
253 measurements. By providing information about the 3-dimensional structure of O_3 and NO_2 the
254 aircraft measurements have played a key role in evaluating the fidelity of air quality forecast
255 model predictions during LMOS.

256 *Other mobile platforms.*

257 Three additional surface-based mobile platforms operated during LMOS 2017: (1) The
258 Geospatial Monitoring of Air Pollution (GMAP) mobile vehicle sampled ozone in transects
259 parallel and perpendicular to the shore. (2) Mobile meteorological and ozone sampling was
260 performed by the UW-Eau Claire team. (3) An instrumented research ship operated out of
261 Sheboygan, WI, with daily measurements of a number of relevant chemical and meteorological
262 parameters. The UW-Eau Claire (UWEC) and EPA Region-5 GMAP vehicle-based samplers
263 operated between the south and north EM sites. These measurements play a key role in
264 determining the distribution of coastal ozone enhancements between the regulatory monitors, the
265 inland penetration of the ozone enhancements, and the timing of the ozone increases along the
266 shoreline.

267 *Forecasting.*

268 Daily forecasting for flight planning purposes utilized WRF-Chem v.3.6.1 at 4-km horizontal
269 resolution (University of Iowa), as well as the operational air quality forecasts from the National
270 Weather Service (NWS) National Air Quality Forecasting Capability
271 (https://airquality.weather.gov/ and
272 https://www.weather.gov/sti/stimodeling_airquality_predictions). The operational forecast is

based on the 12-km North American Model (NAM) meteorology and CMAQ (photochemical grid model, v.5.0.2).

Meteorological and Air Quality Context

The LMOS 2017 sampling period, 22 May through 22 June, captured a typical increase in spring temperatures with periodic rainfall, regular lake breezes and three distinct high pollution episodes. Figure 3 summarizes key meteorological and air pollution variables for LMOS 2017. The LMOS 2017 team identified three episodes with high ozone concentrations for more detailed study, shown in Figure 3b. Classification of days is discussed in detail in Doak et al. (2021), and generally required one or more routine ozone monitoring sites along the western shore of Lake Michigan to register a maximum daily 8-hour average (MDA8) ozone concentration of 70 ppb or higher. The first period, extending from 2 to 4 June, had highest ozone concentrations on 2 June at both Sheboygan KA and Zion for the entire study period. The second and third episodes occurred 9-12 June and 14-16 June, respectively. During the ozone episodes, formaldehyde (Fig. 3c), fine aerosol mass (Fig. 3d), and organic aerosols (Fig. 3d) also increase.

The frequency of high MDA8 ozone concentrations at Zion and Sheboygan KA was similar to climatological averages for the study period. Climatology frequencies for events exceeding 85 ppb are 1 or less during the field campaign weeks of the year; the most severe ozone episode during LMO2017 did not reach that threshold.

Characterization of synoptic meteorology influences on air quality during LMOS 2017 was conducted by inspection of weekly anomalies in temperature, pressure, and precipitation fields of the North American Regional Reanalysis (Mesinger et al. 2006), and by consulting the NOAA National Centers for Environmental Information synoptic discussions for May and June 2017

(NOAA NCEI, 2017a; NOAA NCEI, 2017b). In general, May 2017, including the first 10 days of the campaign at the end of the month, were wetter and colder than climatological average conditions for Wisconsin and northeastern Illinois. These cold and wet conditions were related to a large amplitude trough over the Northern Plains. Figure 3 shows campaign measurements consistent with these synoptic conditions – rainy with cool temperatures, low ozone concentrations, depressed biogenic primary and secondary hydrocarbon concentrations, and low aerosol concentrations.

As the trough over the Northern Plains moved to the northeast during the second week of the campaign (28 May – 3 June), the weather became warmer, drier, and generally windier — coincident with ozone episode A. During the third week of the campaign (4–11 June), a weak ridge dominated the central plains leading to slightly above-average temperatures over southern and central Wisconsin.

During the fourth week of the campaign (12–19 June), a large-amplitude ridge over the central and eastern U.S. led to above average temperatures over Iowa, Wisconsin, Michigan, and northern Illinois. Ozone episodes B and C occurred during this period of warm weather and generally southerly winds (end of third week and middle of fourth week). The relative amount of biogenic compounds (isoprene, MVK, MACR) increase relative to anthropogenic compounds (BTEX), marking a transition from low biogenic conditions (prior to 4 June) to higher biogenic conditions (after 12 June). This transition and its effect on aerosol particles (Figs. 3c and 3d), is discussed in more detail in Hughes et al. (2021).

In addition to being conducive for ozone formation and transport, the warm and humid conditions in northeastern Wisconsin resulted in increased afternoon cloudiness and occasional thunderstorms (see rainfall in Figure 3a where there was some rainfall in the study area every

day starting 12 June). This complicated flight planning on behalf of the airborne passive remote sensing platform and led to heterogeneous spatial and temporal patterns in air pollutants relative to clear sky episodes. The final week of the campaign had below-normal temperatures over Minnesota and northwestern Wisconsin and near-normal temperatures in Illinois, producing strong surface temperature gradients and somewhat stronger westerly winds over eastern Wisconsin and east-central Illinois. As shown in Figure 3b, ozone concentrations were fairly low during this period.

Ozone pollution roses at Sheboygan KA are shown in Figure 4 as derived from observations (left) and from the NOAA National Weather Service Operational NAM-CMAQ forecast. The highest ozone concentrations (>60 ppb) were most commonly observed when winds are from the south or southwest (lake breeze). At Sheboygan KA, the shoreline is angled, running about 35° clockwise of a pure north-to-south line; therefore, at Sheboygan KA, winds from the south and SSW approach from over the lake. Principal errors of the NWS NAM-CMAQ forecasts include both the failure to forecast the frequency of lake breeze circulations at Sheboygan KA, and a large underestimate in peak ozone concentrations.

Featured Measurements

A. Quantifying Weekday/Weekend Emission variability

GeoTASO raster pattern flights, in combination with continuous Pandora measurements, enabled emissions characterization by observing the spatial and temporal variations in NO_2 columns during LMOS 2017. (set SIDEBAR box here) One stark example of this variability is provided by consecutive morning measurements from Sunday, 18 June, and Monday, 19 June,

Accepted for publication in *Bulletin of the American Meteorological Society*. DOI 10.1175/BAMS-D-20-0061.1.

that highlight the weekend-to-weekday transition. Figure 5 shows spatial maps of NO_2 column abundances during the morning (0730–0930 CST; 1330–1530 UTC) on Sunday and Monday over Chicago from GeoTASO. Wind speeds at Chicago Midway ranged from 5 to 9 m s^{-1} on 18 June and 3 to 6 m s^{-1} on 19 June and were predominately from the west to WSW on both days. These GeoTASO measurements show strong signatures of weekday enhancements with peak tropospheric NO_2 columns of (5–6) x 10^{15} molec cm^{-2} on Sunday, 18 June, and over 20 x 10^{15} molec cm^{-2} on Monday, 19 June. Diurnal time series of NO_2 total column abundances from Pandora measurements located at the Schiller Park monitoring station show that the enhancement observed by GeoTASO on the morning of Monday, 19 June, is associated with the morning rush hour, which peaks between 0600 and 0900 CST. The absence of this peak the day before, along with much lower GeoTASO NO_2 signal, suggests that these enhancements are consistent with weekday-associated emissions that are absent or much lower on the weekend. Combined, these GeoTASO and Pandora measurements provide valuable constraints on NO_2 emission inventories used for air quality forecasting and assessment modeling.

B. Spatial Characterization of an Ozone Exceedance

In situ airborne measurements add additional horizontal and vertical characterization of the distribution of NO_2 and of the relationship between NO_2 and ozone enhancements over Lake Michigan. These measurements also provide data for evaluation of photochemical grid model performance and the GeoTASO NO_2 column retrievals. Figure 6 highlights data from 2 June, which was one of the major coastal ozone exceedance days sampled during the 2017 LMOS campaign (also see Figure 3). On this day GeoTASO reveals elevated on-shore and off-shore tropospheric NO_2 columns over Milwaukee and north of Zion that extend out over Lake Michigan, as well as a narrow plume of enhanced tropospheric NO_2 column that extends to the

364 northwest of Sheboygan that is associated with emissions from the Edgewater Power Plant. The
365 spatial pattern between the GeoTASO tropospheric NO_2 columns and the integrated SA NO_2
366 profiles are similar that afternoon. Slight difference of up to 2 x 10^{15} molec cm^{-2} is within the
367 uncertainty of the GeoTASO retrieval and these samples are not entirely temporally co-located
368 as is annotated in the Figure 6A.

369 The order of the SA spirals are indicated by the red arrows in Figure 6A. Off-shore spirals
370 near Sheboygan and Zion occurred during the north-to-south transect. The on-shore spirals over
371 Zion, off-shore spirals near Milwaukee, and on-shore spirals near Sheboygan occurred during the
372 south-to-north transects. Low-level legs were conducted off-shore of Milwaukee during both the
373 north-to-south and south-to-north transects. SA observations show that ozone mixing ratios
374 exceed 100–110 ppb below 100-m altitude off-shore of Milwaukee; near Zion, ozone mixing
375 ratios are near 100 ppb between 200-m and 400-m altitude.

376 The largest ozone enhancements offshore of Milwaukee are not captured by the 4-km WRF-
377 Chem simulation. The 4-km WRF-Chem simulations predict ozone mixing ratios of up to 70 ppb
378 on the earlier north-to-south transects and up to 80 ppb on the later south-to-north transect,
379 reflecting ozone production during this time period between the first spiral at 1307 CST and
380 1743 CST. SA observations show NO_2 >10 ppb off-shore of Milwaukee during low-level legs of
381 both transects that are also not captured by the 4-km WRF-Chem simulation. Short duration
382 decreases in NO_2 at intermediate altitudes (near 200 m) are also observed by SA and not
383 reproduced in WRF-Chem. The significant underestimate of both ozone and NO_2 relative to the
384 SA measurements within the marine boundary layer off-shore of Milwaukee, and the general
385 ozone underestimate by the 4-km WRF-Chem simulation, highlight the difficulties in predicting
386 shoreline ozone exceedances along the western shore of Lake Michigan.

387 *C. High Temporal Observations of the Lake Breeze*

388 Lake breezes are an important component of air pollution meteorology around Lake
389 Michigan, and one of the study objectives was to characterize them in detail, including vertical
390 profiling. The criteria for identifying lake breezes are a shift in surface wind direction from
391 offshore to onshore that was nearly-coincident with an abrupt cooling of surface temperatures
392 and a rapid decrease in thermodynamic mixing height. In addition, cases with precipitation
393 within 3 hours of the wind shift are excluded. Using these criteria, five lake breezes are clearly
394 identified at both of the EM sites (Wagner et al., 2021). As shown by the bold and underlined
395 wind directions in Figure 3, these occur on 2, 8, 11, 12 and 16 June. Lake breezes also occur at
396 Zion on 15 June and at the Sheboygan site on 17 June. The average lake breeze arrival time is
397 0932 CST at the Sheboygan site, and 1030 CST at Zion.

398 The cases examined are generally characterized by weak synoptic forcing and light winds.
399 Three time series from the 2 June event are shown in Figure 7. Winds at Zion are observed by
400 sodar between 30 and 200 m AGL; winds shift direction abruptly at all observed levels (Fig. 7a)
401 as surface temperatures decrease (Fig. 7c) with arrival of the lake breeze. Wind observations at
402 the Sheboygan site from Doppler lidar begin at about 140 m AGL. Though the lidar does not
403 capture the onshore flow at lower levels, Figure 7b shows the upward growth of the lake breeze
404 about two hours after arrival at the surface. For the set of cases examined, the depth of the
405 onshore flow grows as the day progressed. Lake breeze arrival is also accompanied by increases
406 in surface relative humidity, decreases in the water vapor mixing ratio, and increases in $PM_{2.5}$
407 concentrations resulting from increases in both Aitken and accumulation mode particles.

408 Abdi-Oskouei et al. (2020) report mixed success in simulating lake breezes during LMOS
409 2017. In 4-km WRF-Chem modeling re-initialized daily with HRRR meteorological fields, good

statistical performance was achieved compared to traditional benchmarks for wind speed, wind direction, temperature, and water vapor mixing ratio. However, model performance for lake breeze was inconsistent, with some days reproduced in fine details and other lake breezes missed. For Sheboygan, wind direction and speed shifts in WRF-Chem followed observed Doppler lidar patterns on all of the lake breeze days, but with errors in timing on some days and insufficient inland penetration on 11 June. For Zion, the model followed wind direction and speed shifts observed by sodar on all of the lake breeze observation days except 11 and 12 June. The failure of the WRF-Chem model to develop lake breeze on 12 June is also discussed in section D. Errors in timing, usually the model being too late in lake breeze onset by 1-2 hours, were common. More detailed analysis of 2 and 11 June, including quantitative metrics, are reported in Abdi-Oskouei et al. (2020). Simulation of lake breeze was found to be necessary but not sufficient for correct simulation of ozone concentrations at coastal sites on most ozone episode days.

D. Coastal Gradient Significance

The GMAP vehicle contained a regulatory-grade commercial ozone monitor and performed pre-planned driving routes to map ozone gradients parallel and perpendicular to the coast. The 12 June drive (episode period B), shown in Figure 8, depicts several features of interest illustrating how the ozone events unfold, the importance of the lake breeze, and the difficulty of forecast modeling at high spatio-temporal resolution. The drive began in late morning and continued south-to-north until late afternoon. Ozone concentrations sampled by the mobile platform generally increased during the day, and ranged from 40 to 89 ppb. Figure 8 shows the path of the drive, color coded by ozone concentration. The strong east-west gradient, most evident at Kenosha, is caused by a shallow lake breeze. The elevated ozone is confined to a narrow band

near the lake shore. The minimum ozone (40.3 ppb) was found at a traffic intersection in Zion (1121 CST). The maximum ozone (89.4 ppb) was found between Kenosha and Racine (1358 CST), less than 200 m from the shoreline. In general, the distance of inland penetration of the lake breeze increased over this period.

The gradient during the Kenosha east-west transect is particularly striking, with ozone levels of just 57.4 ± 1.6 ppb (± one standard deviation) at distances more than 4.1 km from the shore. These can be contrasted with 81.4 and 87.4 ppb, respectively, at the beginning and end of the transect (closest to the shore). The gradient during the later (eastbound) portion of the transect is about 9 ppb km^{-1} over a 3.15-km distance. In other words, ozone varies by over 27 ppb within one model grid cell. The primary reason for the gradient is the limited inland penetration of the ozone-rich lake breeze. At the end of the drive, at Racine (1323 CST), the inland penetration distance has increased, leading to a decrease in the strength of the ozone gradient.

The WRF-Chem model output, shown in Figure 8b, exhibits a good match with the inland portions of the drive where ozone is 40–60 ppb during the earlier (southern) east-west transect. Specifically, in the portion of the drive corresponding to the southernmost three grid cells, the observed and modeled ozone are 54.3 and 59.1 ppb, respectively. The simulation produces elevated ozone (up to 87.4 ppb) over the lake, but transport patterns are such that it does not reach the GMAP drive locations. Analysis in Abdi-Oskouei (2020) explores the role of lake breeze and synoptic wind in positioning the ozone plume of 12 June. Figure 8b highlights the challenge of model reproduction of fine spatio-temporal features in coastal ozone. In order to reproduce the timing and magnitude of the ozone time series at coastal monitors, ozone production over the lake must be correctly simulated; furthermore, details of the lake breeze must be accurate – timing, horizontal extent, and vertical structure.

LMOS 2017 Findings

LMOS 2017, an observational field campaign focused on elevated ozone over Lake Michigan and the associated meteorology, ozone precursors, and oxidant chemistry, was successful in capturing relevant events. Three high ozone episodes were captured: 2–4 June, 9–12 June, and 14–16 June. The rich set of in situ and remotely sensed measurements collected during LMOS highlight the complex chemistry and meteorology that leads to ozone production along the western shore of Lake Michigan. These datasets resulted in valuable findings on their own but also serve as a guidepost to assess credibility of models and their representation of these complex photochemical and dynamical processes.

LMOS 2017 aircraft observed narrow plumes of high ozone and nitrogen dioxide (NO_2) concentrations within the marine boundary layer over Lake Michigan, at altitudes ranging from about 50 to 370 m above lake level depending on date, time of day, and location. These measurements point to the need for air quality models to have high vertical resolution within the shallow marine boundary layer to adequately capture the vertical structure of mixing and photochemistry as the pollution plumes are transported over the lake.

GeoTASO remote sensing of NO_2, supported by ground-based Pandora remote sensing (Judd et al., 2019) and in situ aircraft profiling, provided unprecedented mapping of NO_2 over the study region, which provides new insight into the impact of satellite footprint sizes on NO_2 column retrievals. This information is critical for use of these remotely sensed airborne, ground based, and satellite NO_2 columns for top-down estimates of emissions inventories.

At the Sheboygan and Zion sites, valuable meteorological datasets were collected, including remote-sensed wind and temperature profiles that provide a detailed observational constraint on the evolution of the lake breeze (Fig. 3a, Fig. 7). At the Sheboygan site, vertical profiles of water vapor and aerosol were also recorded. These measurements can be used to improve the meteorological predictions of lake breeze circulations which are necessary to predict coastal ozone enhancements in this region.

Elevated ozone periods were predominantly, but not completely, associated with lake breeze airflow. Six lake breeze events have been identified at each of the EM sites and analyzed in detail for temporal features and connections between surface observations and the vertical profiles. An example of the sensitivity of concentrations to horizontal penetration depth of the lake breeze is shown in Figure 8 as observed from GMAP.

LMOS 2017 shows that ozone air pollution can occur during both anthropogenically-dominant periods (prior to 4 June) and during periods when both anthropogenic and biogenic emissions are significant (after 9 June). The transition between these two periods is apparent in time series of concentrations of NO_x, formaldehyde, aerosol tracer species, anthropogenic VOCs, isoprene, and isoprene oxidation products.

Contemporary PGM models capture many features of air pollution and meteorology well during LMOS 2017 (e.g., the MDA8 temporal variability in Figure 3b, the directional dependence of high ozone in Figure 4, diel patterns of many species, and average spatial patterns of ozone MDA8). However, two classes of ozone simulation difficulties persist: airshed-wide bias on exceedance days (e.g. Figs. 3b, 6b, 6d, & 8), and consistent reproduction of fine spatio-temporal features (narrow plumes, vertically shallow layers, lake breeze inland penetration distance and timing, and NO_2 and other ozone precursors in lake breezes). Using both in situ

airborne and surface ozone measurements, we find that both the NAM-CMAQ 12-km modeling and the higher resolution (4-km) WRF-Chem modeling underestimate peak ozone concentrations and overestimate NO_2 concentrations during ozone episodes. Model observation differences are reduced but persist in post-analysis modeling with improved meteorological fields. Statistics for WRF-Chem O_3 MDA8 on days with observed MDA8 above 65 ppb (n=6) are: biases of -4.6 and -10.2 ppb, respectively, at Zion and Sheboygan KA (graphed in Figure 3b). On low ozone days, a positive bias was found in WRF-Chem modeling at these two sites; ozone bias stratified by ozone MDA8 can be found in supplemental material. For the NAM-CMAQ model (Figure 4), ozone above 60 ppb is much more common in observations than in the model (12.5 and 6.2 times more common, respectively, at Sheboygan KA and Chiwaukee Prairie). NO_2 is overpredicted in NAM-CMAQ relative to aircraft observations below 500 m by a factor of 2-4 (0.2-1 ppb interquartile range in observation, and 1-3.5 ppb interquartile range in model). Performance of modeled NO_2 compared to aircraft in situ profiles, reported in Abdi-Oskouei et al. (2019), is similar to that of NAM-CMAQ. Additionally, both modeling systems underpredict NO_2 at altitudes above about 2 km.

Further model sensitivity studies exploring emissions sensitivities, model resolution, model physics, and model chemical mechanisms need to be conducted to further quantify the reasons for these discrepancies so that they can continue to be reduced. For example, ongoing WRF physics sensitivity studies by the LMOS team suggest that the ability to capture the inland penetration of the lake breeze circulation is dependent on accurate estimates of the Lake Michigan water temperatures, soil moisture, model resolution, and the physics options chosen to represent boundary layer mixing and land surface exchange processes. Both Abdi-Oskouei et al. (2020) and McNider et al. (2018) found important influence of land surface models and data

assimilation for land and atmospheric conditions. Abdi-Oskouei et al. (2020) found improvement in meteorological variables with the Noah land surface model (Chen and Dudhia, 2001) and with initialization to the 3- km High- Resolution Rapid Refresh (HRRR) (Benjamin et al., 2016) while McNider found best meteorological performance when assimilating insolation, satellite-derived vegetative greenness, and other land surface characteristics.

Ozone sensitivity to NO_x and VOC was assessed through indicator chemical ratios (formaldehyde and NO_2 at Sheboygan; H_2O_2 and HNO_3 at Zion) supplemented by box modeling. The results suggest a complex system with some NO_x limited periods, and some VOC limited periods. Discussion of the chemistry, emissions sensitivity, and HO_x radical fates on 2 June can be found in Vermeuel et al. (2019) while the aerosol chemistry of the event is discussed in Hughes et al. (2021) and indicator ratios at the Sheboygan site are discussed in Abdi- Oskouei et al. (2019). Findings are most developed for 2 June within episode A. For 2 June, Vermeuel et al. (2019) conducted detailed Lagrangian box modeling. On that day, airflow went from Chicago (early morning), out over the lake, and finally to Zion (16:00 CST). Ozone production peaked at solar noon at a rate of 10 ppb h^{-1}. Conditions were initially strongly VOC limited. The degree of VOC limitation decreased during the evolution of the plume but remained VOC sensitive when this airmass moved onshore and was detected by instruments at the Zion EM site.

Each ozone event observed during LMOS 2017 was different. We believe these differences are significant for air quality model evaluation, future field campaign design, and air quality management. For example, the H_2O_2/HNO_3 ratio during the 2 June ozone event at Zion (0.35) event was much lower than the study average of 3.3 (Vermeuel et al. 2019). Other observational and model-based lines of evidence support the variation in ozone event chemistry and meteorology. For example, 2 June occurred within the anthropogenically dominated portion of

the campaign; modeled ozone concentrations at Zion on 2 June were highly sensitive to anthropogenic VOC emissions in Chicago as would be expected in a NO_x rich plume. Finally, the 2 June ozone event had unique $PM_{2.5}$ composition at Zion – with a strong primary combustion source influence (Hughes et al. 2021).

In addition to variability in NO_x-VOC sensitivity, the ozone episodes vary in other aspects, including the importance of biogenics and the role of background and long-distance transport of ozone and ozone precursors. For example, the 11 June event differed from that on 2 June in terms of both aerosol chemistry and predominant air mass origin. On 11 June, high levels of organosulfates derived from isoprene oxidation were detected (Hughes et al. 2021). The source region was likely forested regions of Missouri and Arkansas. This air mass, transported over a relatively long distance, interacted with local emissions to contribute to the 9–12 June episode.

One finding from LMOS 2017 is that the conceptual model of a NO_x rich and VOC sensitive urban core zone of high ozone production is useful. As plumes photochemically age, sensitivity of ozone production shifts – usually to a balanced regime where there is sensitivity to both NO_x and VOC. The strength of the initial VOC sensitivity in the urban plume, and the location where the transition occurs, vary from episode to episode. This general pattern and associated variability from episode to episode should be kept in mind for future work on ozone air quality in the Lake Michigan airshed.

Another lesson learned from the analysis of LMOS 2017 data is that future campaigns need enhanced VOC measurements in source regions. A denser spatial network of high temporal resolution VOC sampling locations is needed. Measurements of both meteorology and chemistry of the urban plumes over the lake would be of great benefit to further development and

Accepted for publication in *Bulletin of the American Meteorological Society*. DOI 10.1175/BAMS-D-20-0061.1.

evaluation chemical transport models for ozone applications at urban-influenced coastal environments such as Lake Michigan.

Acknowledgements

The LMOS 2017 Science Team acknowledges the NASA Airborne Science Program and the NASA GEOstationary Coastal and Air Pollution Events (GEO-CAPE) Mission Pre-formulation Science Working Group for supporting the airborne remote sensing instruments. This work was funded in part by the National Science Foundation under collaborative grants AGS- 1712909 (COS, EAS), AGS- 1713001 (THB), and AGS- 1712828 (DBM). DBM also acknowledges support from NSF under grant AGS-1428257, and EAS acknowledges support from AGS-1405014. The UW Eau Claire team acknowledges the Student Blugold Commitment Differential Tuition program, and NSF award 1400815. We acknowledge EPA and the NOAA GOES-R program office for supporting the measurements at Sheboygan, and the Electric Power Research Institute (EPRI) for supporting the Scientific Aviation airborne measurements. The University of Iowa modeling team acknowledges NASA support under NNX16AN36G.

We would like to acknowledge the strong support of EPA's Office of Research and Developments A-E-Energy Research Program in the design and execution of LMOS. We would specifically like to thank Robert Kaleel, former direct of LADCO, for initial contributions to LMOS 2017. We also thank the team at Scientific Aviation, Donald R. Blake (UC Irvine, for VOC analyses), Michal Derliki, Andrew Habel, and Keith Kronmiller with the EPA support contractor Jacobs, and Nishanthi Wijekoon of Wisconsin DNR for mapping support and data.

Any opinions, findings, and conclusions or recommendations expressed in this material are those of the author(s) and do not necessarily reflect the views of the National Science Foundation nor should they be construed as an official National Oceanic and Atmospheric Administration or U.S. Government position, policy, or decision. The views expressed in this paper are those of the authors and do not necessarily represent the views or policies of the U.S. Environmental Protection Agency. EPA does not endorse any products or commercial services mentioned in this publication.

Data Availability Statement

Measurements used herein are available at the NASA data repository (https://www-air.larc.nasa.gov/cgi-bin/ArcView/lmos). Model fields used herein are available upon request of the corresponding author.

Accepted for publication in *Bulletin of the American Meteorological Society*. DOI 10.1175/BAMS-D-20-0061.1.

603 *References Cited*

604

605 Abdi-Oskouei, M., and Coauthors, 2020: Sensitivity of Meteorological Skill to Selection of
606 WRF-Chem Physical Parameterizations and Impact on Ozone Prediction During the Lake
607 Michigan Ozone Study (LMOS). *Journal of Geophysical Research-Atmospheres*, **125,**
608 25, https://doi.org/10.1029/2019jd031971.
609 Abdi-Oskouei, M., and Coauthors, 2019: Lake Michigan Ozone Study (2017) Preliminary
610 Finding Report.
611 Adelman, Z., cited 2020: LADCO Public Issues. Available online at
612 https://www.ladco.org/public-issues/.
613 Benjamin, S. G., and Coauthors, 2016: A North American Hourly Assimilation and Model
614 Forecast Cycle: The Rapid Refresh. *Monthly Weather Review*, **144,** 1669-1694,
615 https://doi.org/10.1175/mwr-d-15-0242.1.
616 Chen, F., and J. Dudhia, 2001: Coupling an advanced land surface-hydrology model with the
617 Penn State-NCAR MM5 modeling system. Part I: Model implementation and sensitivity.
618 *Monthly Weather Review*, **129,** 569-585.
619 Cleary, P. A., and Coauthors, 2015: Ozone distributions over southern Lake Michigan:
620 Comparisons between ferry-based observations, shoreline-based DOAS observations and
621 model forecasts. *Atmos. Chem. Phys.*, **15,** 5109-5122, https://doi.org/10.5194/acp-15-
622 5109-2015.
623 Doak, A. G., and Coauthors, 2021: Characterization of ground-based atmospheric pollution and
624 meteorology sampling stations during the Lake Michigan Ozone Study 2017. *Journal of*
625 *Air and Waste Management (in press)*, https://doi.org/10.1080/10962247.2021.1900000.

626 Dye, T. S., P. T. Roberts, and M. E. Korc, 1995: Observations of transport processes for ozone
627 and ozone precursors during the 1991 Lake Michigan Ozone Study. *Journal of Applied*
628 *Meteorology*, **34,** 1877-1889.
629 Fishman, J., and Coauthors, 2008: Remote sensing of tropospheric pollution from space. *Bull.*
630 *Amer. Meteorol. Soc.*, **89,** 805-821, https://doi.org/10.1175/2008bams2526.1.
631 Fishman, J., and Coauthors, 2012: The United States' next generation of atmospheric
632 composition and coastal ecosystem measurements NASA's Geostationary Coastal and Air
633 Pollution Events (GEO-CAPE) Mission. *Bull. Amer. Meteorol. Soc.*, **93,** 1547-1566,
634 https://doi.org/10.1175/bams-d-11-00201.1.
635 Foley, T., E. A. Betterton, P. E. Robert Jacko, and J. Hillery, 2011: Lake Michigan air quality:
636 The 1994-2003 LADCO Aircraft Project (LAP). *Atmos. Environ.*, **45,** 3192-3202,
637 https://doi.org/10.1016/j.atmosenv.2011.02.033.
638 Good, G., 2017: Supplemental Information for 2015 Ozone National Ambient Air Quality
639 Standard (NAAQS) Area Designations.
640 Hughes, D. D., and Coauthors, 2021: PM2.5 chemistry, organosulfates, and secondary organic
641 aerosol during the 2017 Lake Michigan Ozone Study. *Atmos. Environ.*, **244,** 117939,
642 https://doi.org/10.1016/j.atmosenv.2020.117939.
643 IGACO, 2004: The changing atmosphere: An integrated global atmospheric chemistry
644 observation. Report of the Integrated Global Atmospheric Chemistry Observation Theme
645 Team, GAW Rep. 159 (WMO/TD-1235), ESA SP-1282.
646 Judd, L. M., and Coauthors, 2018: The Dawn of Geostationary Air Quality Monitoring: Case
647 Studies From Seoul and Los Angeles. *Front. Environ. Sci.*, **6,** 17,
648 https://doi.org/10.3389/fenvs.2018.00085.

Judd, L. M., and Coauthors, 2019: Evaluating the impact of spatial resolution on tropospheric NO2 column comparisons within urban areas using high-resolution airborne data. *Atmos. Meas. Tech.*, **12,** 6091–6111, https://doi.org/10.5194/amt-12-6091-2019.

Knuteson, R. O., and Coauthors, 2004: Atmospheric emitted radiance interferometer. part I: Instrument design. *Journal of Atmospheric and Oceanic Technology*, **21,** 1763-1776, https://doi.org/10.1175/jtech-1662.1.

Kowalewski, M. G., and S. J. Janz, 2014: Remote sensing capabilities of the GEO-CAPE airborne simulator. Proc. SPIE 9218, *Earth Observing Systems XIX*, 92181I, https://doi.org/10.1117/12.2062058.

Laird, N. F., D. A. R. Kristovich, X. Z. Liang, R. W. Arritt, and K. Labas, 2001: Lake Michigan lake breezes: Climatology, local forcing, and synoptic environment. *Journal of Applied Meteorology*, **40,** 409-424.

Leitch, J. W., and Coauthors, 2014: The GeoTASO airborne spectrometer project. Proc. SPIE 9218, *Earth Observing Systems XIX*, 92181H, https://doi.org/10.1117/12.2063763

Lennartson, G. J., and M. D. Schwartz, 2002: The lake breeze-ground-level ozone connection in eastern Wisconsin: A climatological perspective. *International Journal of Climatology*, **22,** 1347-1364, https://doi.org/10.1002/joc.802.

Levelt, P. F., and Coauthors, 2018: The Ozone Monitoring Instrument: overview of 14 years in space. *Atmos. Chem. Phys.*, **18,** 5699-5745, https://doi.org/10.5194/acp-18-5699-2018.

Lyons, W. A., and L. E. Olsson, 1973: Detailed mesometeorological studies of air pollution dispersion in the Chicago lake breeze. *Monthly Weather Rev.*, **101,** 387-403.

Makar, P. A., and Coauthors, 2010: Dynamic adjustment of climatological ozone boundary conditions for air-quality forecasts. *Atmos. Chem. Phys.*, **10,** 8997-9015, https://doi.org/10.5194/acp-10-8997-2010.

Mazzuca, G. M., and Coauthors, 2016: Ozone production and its sensitivity to NOx and VOCs: results from the DISCOVER-AQ field experiment, Houston 2013. *Atmos. Chem. Phys.*, **16,** 14463-14474, https://doi.org/10.5194/acp-16-14463-2016.

McBride, B. A., J. V. Martins, H. M. J. Barbosa, W. Birmingham, and L. A. Remer, 2020: Spatial distribution of cloud droplet size properties from Airborne Hyper-Angular Rainbow Polarimeter (AirHARP) measurements. *Atmos. Meas. Tech.*, **13,** 1777-1796, https://doi.org/10.5194/amt-13-1777-2020.

McNider, R. T., and Coauthors, 2018: Examination of the Physical Atmosphere in the Great Lakes Region and Its Potential Impact on Air Quality – Overwater Stability and Satellite Assimilation. *Journal of Applied Meteorology and Climatology*, **57,** 2789-2816, https://doi.org/10.1175/jamc-d-17-0355.1.

Mesinger, F., and Coauthors, 2006: North American regional reanalysis. *Bull. Amer. Meteorol. Soc.*, **87,** 343-360, https://doi.org/10.1175/bams-87-3-343.

Miller, P., 2018: A34B-01: Overview of the Long Island Sound Tropospheric Ozone Study (LISTOS). *Annual Meeting of the AGU*.

NOAA NCEI (National Centers for Environmental Information), 2017a, State of the Climate: Synoptic Discussion for May 2017, published online June 2017, retrieved on May 25, 2021 from https://www.ncdc.noaa.gov/sotc/synoptic/201705.

691 NOAA NCEI (National Centers for Environmental Information), 2017b, State of the Climate:
692 Synoptic Discussion for June 2017, published online July 2017, retrieved on May 25,
693 2021 from https://www.ncdc.noaa.gov/sotc/synoptic/201706.
694 Sullivan, J. T., and Coauthors, 2019: The Ozone Water-Land Environmental Transition Study:
695 An Innovative Strategy for Understanding Chesapeake Bay Pollution Events. *Bull. Amer.*
696 *Meteorol. Soc.*, **100,** 291-306, https://doi.org/10.1175/bams-d-18-0025.1.
697 USEPA, 2006: Air Quality Criteria For Ozone and Related Photochemical Oxidants (Final
698 Report, 2006) EPA/600/R-05/004aF-cF.
699 ——, 2015: Regulatory Impact Analysis of the Final Revisions to the National Ambient Air
700 Quality Standards for Ground-Level Ozone October 1, 2015.
701 ——, 2103: Integrated Science Assessment (ISA) for Ozone and Related Photochemical
702 Oxidants (Final Report, Feb 2013) EPA/600/R-10/076F.
703 Vermeuel, M. P., and Coauthors, 2019: Sensitivity of Ozone Production to NOx and VOC Along
704 the Lake Michigan Coastline. *Journal of Geophysical Research-Atmospheres*, **124,**
705 10989-11006, https://doi.org/10.1029/2019jd030842.
706 Wagner, T. J., P. M. Klein, and D. D. Turner, 2019: A new generation of ground-based mobile
707 platforms for active and passive profiling of the boundary layer. *Bull. Amer. Meteorol.*
708 *Soc.*, **100,** 137-153, https://doi.org/10.1175/bams-d-17-0165.1.
709 Wagner, T. J., A. C. Czarnetzki, M. Christiansen, R. B. Pierce, C. O. Stanier, and E. W. Eloranta,
710 2021: Observations of the Development and Vertical Structure of Lake Michigan Lake
711 Breezes. *Journal of Atmospheric Sciences (in review).*
712 Zhang, J., M. Ninneman, E. Joseph, M. J. Schwab, B. Shrestha, and J. J. Schwab, 2020: Mobile
713 Laboratory Measurements of High Surface Ozone Levels and Spatial Heterogeneity

During LISTOS 2018: Evidence for Sea Breeze Influence. *Journal of Geophysical Research-Atmospheres*, **125,** 12, https://doi.org/10.1029/2019jd031961.

Zoogman, P., and Coauthors, 2017: Tropospheric emissions: Monitoring of pollution (TEMPO). *J. Quant. Spectrosc. Radiat. Transf.*, **186,** 17-39, https://doi.org/10.1016/j.jqsrt.2016.05.008.

SIDEBAR – Preparing for New Air Quality Monitoring Capabilities

The global distributions of air quality (AQ) pollutants have now been observed by satellite instruments (e.g., the Ozone Monitoring Instrument; Levelt et al. 2018) for over two decades, collecting data for monitoring climatologic, economic, and regulatory impacts on air pollution globally. However, these instruments on satellites in low Earth orbits have provided observations at only one time of day, typically the early afternoon. AQ scientists and managers have long advocated for AQ observations from geostationary satellites, necessary for providing information about the "chemical weather" many times per day (IGACO, 2004; Fishman et al., 2008; Fishman et al., 2012). Such observations will help advance capabilities for monitoring and predicting air quality, analogous to how geostationary meteorological observations have become so fundamental within the weather community. This advancement will move forward when NASA launches the Tropospheric Emissions: Monitoring of Pollution (TEMPO) mission in 2022 (tempo.si.edu) providing the first geostationary AQ trace gas observations over greater North America, complementing the aerosol information available from the Advanced Baseline Imager (ABI) on the current generation of GOES satellites. TEMPO observations include key tropospheric pollutants such as nitrogen dioxide (NO_2), formaldehyde, and ozone (O_3) at unprecedented temporal (hourly) and spatial (~2.1 x 4.4 km) resolutions (Zoogman et al., 2017), giving a revolutionary perspective for addressing O_3 air quality challenges. TEMPO is also a component of the developing global integrated AQ observing system, along with two other geostationary missions—South Korea's Geostationary Environment Monitoring Spectrometer (GEMS) launched in February 2020, observing Southeast Asia, and the European Copernicus Programme's Sentinel-4, to be launched in 2023 and observing Europe and Northern Africa.

743 To prepare for the never-before-captured spatial and temporal perspective of geostationary
744 AQ observations, NASA supported the development of airborne instruments similar to TEMPO,
745 GCAS (Kowalewski and Janz, 2014; Leitch et al., 2014) and GeoTASO (Leitch et al., 2014), as
746 well as the ground-based instrument, Pandora (https://pandora.gsfc.nasa.gov/). Working with
747 partners such as the US EPA over the past decade, NASA has deployed these instruments
748 together over multiple regions of the country during air quality studies including LMOS. While
749 satellite data excel at providing information in the gaps of surface measurement frameworks,
750 they must be combined with additional information (including surface in situ concentrations and
751 mixing layer heights) to enhance the relevance of the information to AQ managers. Pandora
752 instruments are increasingly being integrated as long-term measurements within U.S. regulatory
753 monitoring sites to provide this critical bridge between satellite observations and standard AQ
754 measurements. The data collected during studies like LMOS are used to help AQ management
755 prepare for using TEMPO data as soon as it becomes available. Observations of the spatial
756 distribution of ozone precursors such as NO_2 and formaldehyde repeatedly throughout the day in
757 these studies are already altering conceptual models of the impacts of emissions, chemistry, and
758 meteorology on AQ (e.g., Judd et al., 2018). Integrating all these observations with existing
759 ground-based measurements and chemical transport models will enable AQ managers to better
760 address ozone issues that continue to plague certain regions despite improving emissions.
761

762 TABLES

763 **Table 1**. Major measurement platforms and locations for LMOS 2017

Location	Measurement*	Research Institution*
Ground Sites		
Sheboygan site (Spaceport Sheboygan at Sheboygan harbor)	Remote sensing of meteorology (wind speed, wind direction, temperature, water vapor) and aerosol backscatter	UW-Madison
	In situ measurements of pollutants (O_3, NO/NO_2/NO_x, NO_y, formaldehyde)	U.S. EPA ORD
Zion, IL	Remote sensing of meteorology (sodar, microwave radiometer), Aerosol Optical Depth (Aeronet) and 10m meteorology	Univ. Northern Iowa, UW-Madison, Illinois EPA
	In situ and offline chemical & physical measurements Gas phase: NO, NO_2, SO_2, HNO_3, H_2O_2, NMHC (C2–C12), OVOC & VOC (alkenes, aromatics, aldehydes, terpenoids, ketones, nitriles, organic acids, isoprene + oxidation products, etc.), other VOC and NO_x oxidation products (N_2O_5, $ClNO_2$, select organic acids, select organic nitrates) Particle phase: aerosol size distributions; $PM_{2.5}$ mass and composition (water-soluble inorganic Ions (NO_3^-, NH_4^+, SO_4^{2-}), metals, organic carbon , elemental carbon and organic molecular markers).	Univ. Iowa, UW-Madison, Univ. Minnesota
	Routine measurements of ozone	Illinois EPA
Various†	Remote sensing of pollutants by Pandora sun spectrometer, and boundary layer height	U.S. EPA ORD
Sheboygan transect	In situ measurements of ozone at four locations	U.S. EPA ORD
Airborne Platforms		
Lakeshore region	Airborne remote sensing of NO_2 and formaldehyde (GeoTASO)	NASA
	Airborne remote sensing of clouds (AirHARP)	Univ. Maryland, Baltimore County
	Airborne in situ profiling of pollutants and meteorology	Scientific Aviation
Shipboard Platform		
Lake Michigan	In situ measurements of pollutants and meteorology	U.S. EPA ORD
	Remote sensing of pollutants and boundary layer height	U.S. EPA ORD
Mobile Platforms		
Northeast IL and Southeast WI	In situ measurements of pollutants (GMAP)	U.S. EPA Region 5
Grafton to Sheboygan	In situ measurements of ozone and meteorology	UW-Eau Claire

764 * GeoTASO = Geostationary Trace gas and Aerosol Sensor Optimization instrument, AirHARP = Airborne Hyper Angular Rainbow
765 Polarimeter, GMAP = Geospatial Monitoring of Pollutants, UW = University of Wisconsin, EPA = Environmental Protection
766 Agency, ORD = Office of Research and Development, NMHC = Non-methane hydrocarbon

767 † Measurement sites can be found in the supplemental material.

768

769 FIGURES

770

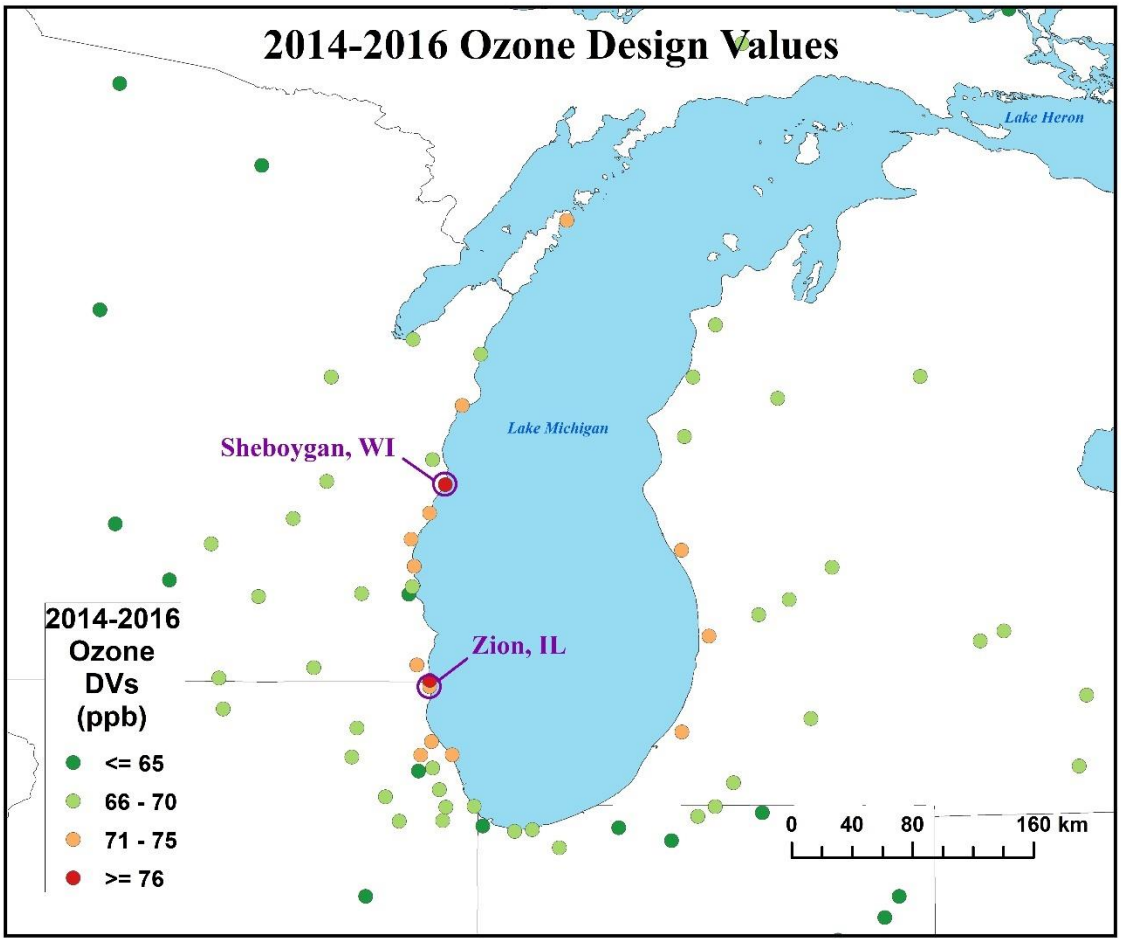

771

772 **Figure 1.** Map of ozone design values (2014–2016) and Lake Michigan Ozone Study 2017
773 (LMOS 2017) ground site locations. Ozone design values (fourth-highest daily monitored 8-hour
774 average ozone concentration at that monitor, averaged over a 3-year period, ppb) for 2014–2016
775 from the U.S. Air Quality System (AQS). Purple circles indicate the primary ground sites hosting
776 measurements for LMOS 2017. Threshold match ozone air quality standards, with 70 ppb as the
777 2015 standard, and 75 ppb as the 2008 standard.

778

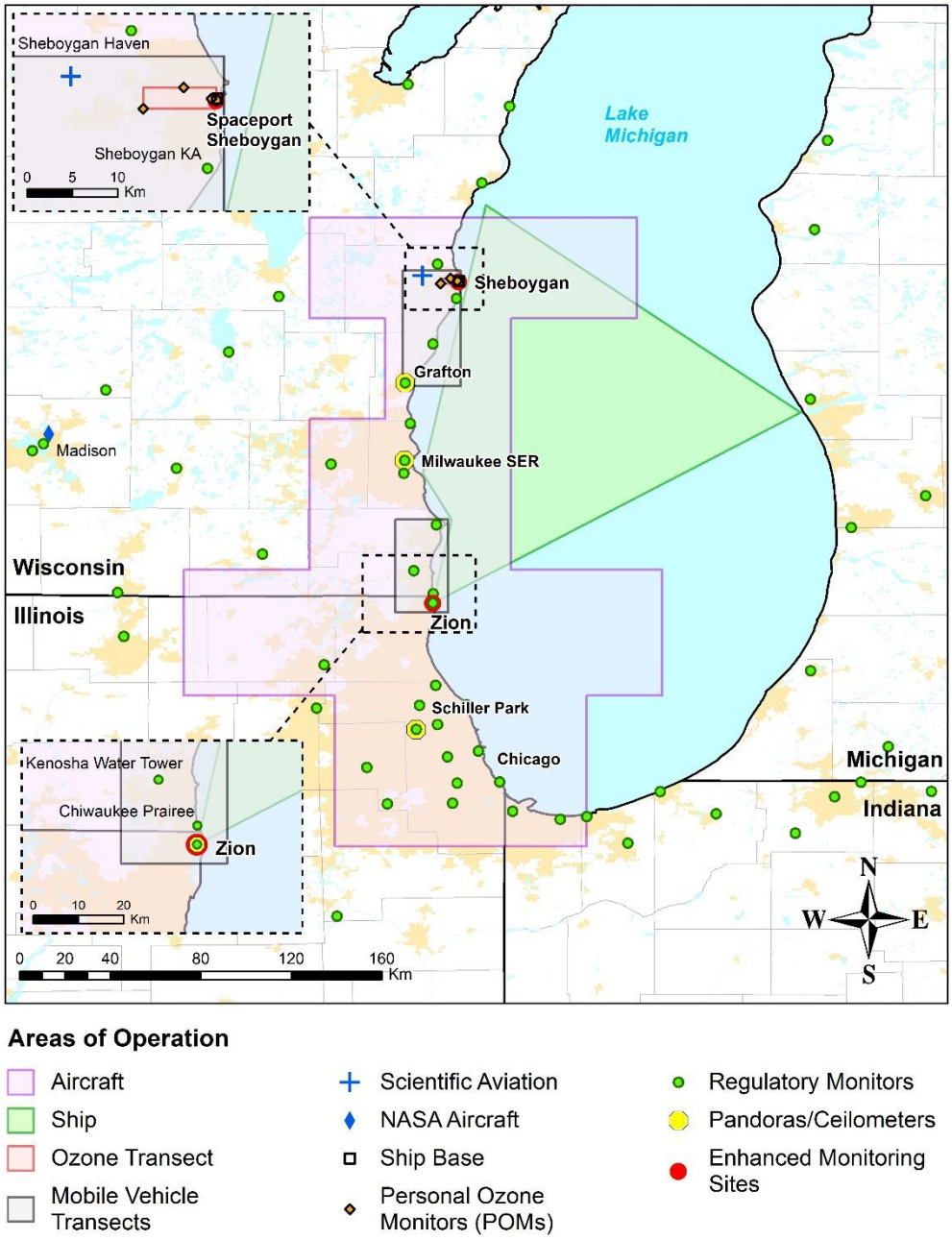

Figure 2. Overview map showing spatial coverage of LMOS 2017 observations. Green and purple polygons indicate ship and aircraft operations areas, respectively. Enhanced monitoring sites at Sheboygan, WI (north) and Zion, IL (south) are mapped in more detail with insets.

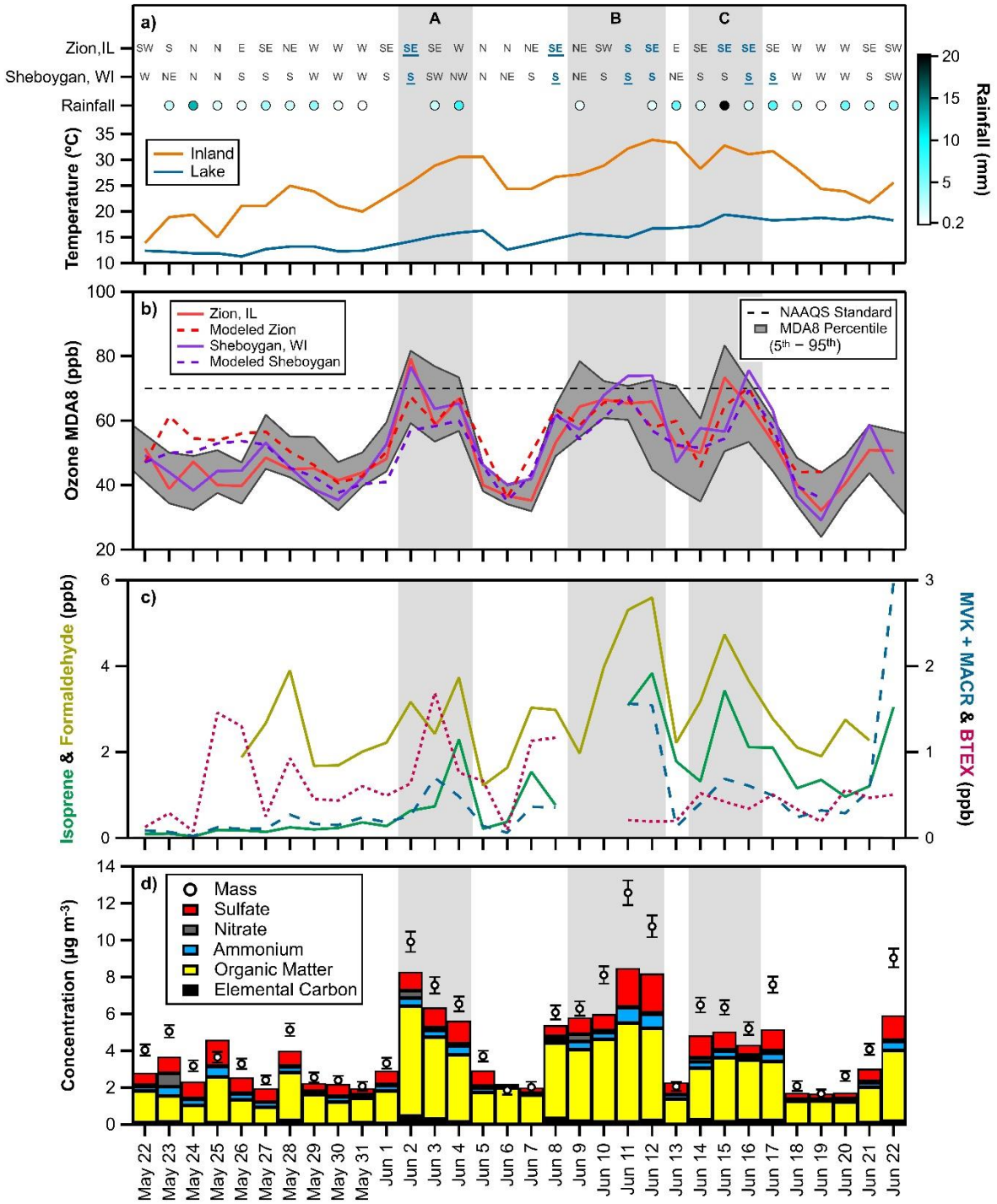

785

786 **Figure 3.** Observational overview of LMOS 2017. Shown are daily time series of (a) winds,

787 rainfall and temperature, (b) ozone MDA8 concentrations, (c) peak hourly concentrations of

788 selected gases, and (d) daytime $PM_{2.5}$ concentrations and chemical composition. Grey vertical

bands indicate ozone episodes. Figure notes: temperatures represent maximum hourly air temperature at Lake Mills, WI, and daily lake water temperature at Wilmette Buoy, IL; wind directions represent the most frequent wind direction during 0800–1600 CST (bold for lake breeze and underlined for deep inland penetration lake breeze); rainfall is the daily total averaged over 27 sites in WI and IL; Sheboygan ozone data are from the KA station; all variables for (c) and (d) are from Zion, IL, except formaldehyde is from the Sheboygan site; gas concentrations are peak hourly values for each day, and (d) is for daytime only (0700–1900 CST).

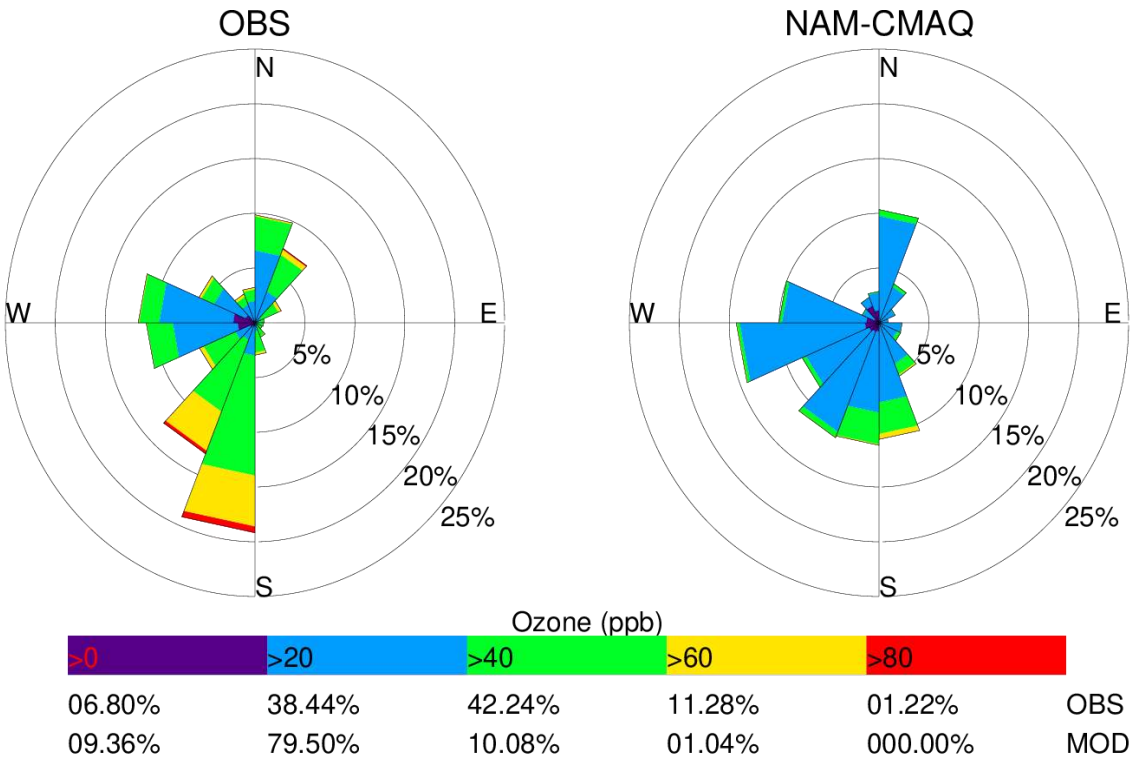

797

798 **Figure 4:** Ozone (ppb) pollution roses based on 1-minute WDNR observations (left) and hourly
799 model output from NAM-CMAQ (right) at the Sheboygan KA from 22 May through 22 June
800 2017. Wind direction frequencies are indicated by the radial distance of the wind rose. The
801 percentage of ozone values falling within 20 ppb bins are indicated by colors for each wind
802 direction. The overall percentages of observed and modeled ozone during LMOS falling in each
803 bin are indicated below the color bars.

804

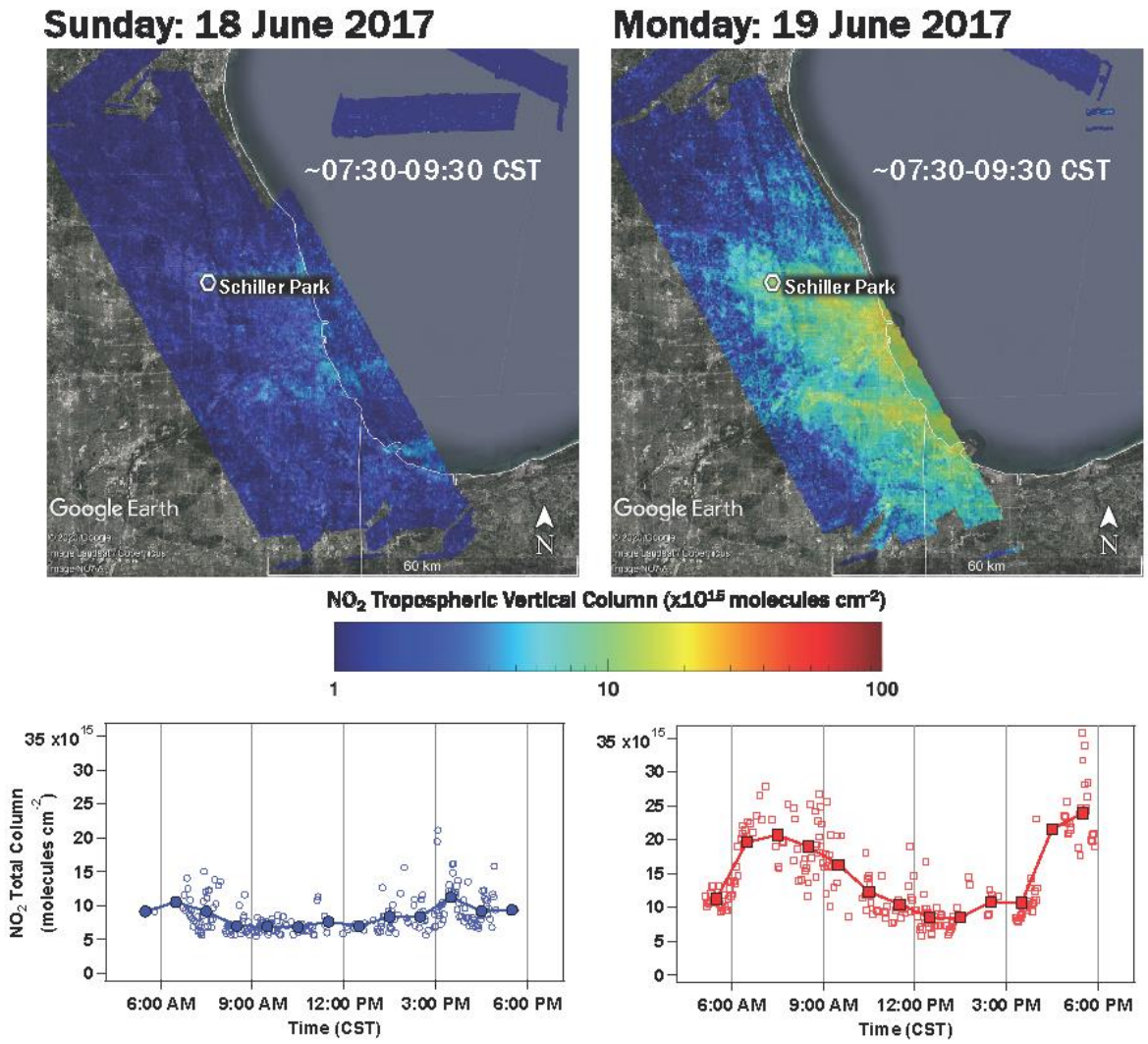

805

806 **Figure 5.** The upper panels show GeoTASO NO_2 Tropospheric Vertical Column Densities

807 (VCD, 10^{15} molec cm^{-2}) from 0730 to 1530 CST on Sunday, 18 June (left) and Monday, 19 June

808 (right), 2017. The location of the Schiller Park AQS monitoring site is labeled. The lower panels

809 show NO_2 Total VCD (molec cm^{-2}) timeseries based on Pandora observations at the Schiller

810 Park AQS station for 18 June (blue, left) and 19 June (red, right), 2017. The Pandora timeseries

are shown as hourly averages (bold symbols) and at the instrument's native temporal resolution (faint symbols), ~88 sec.

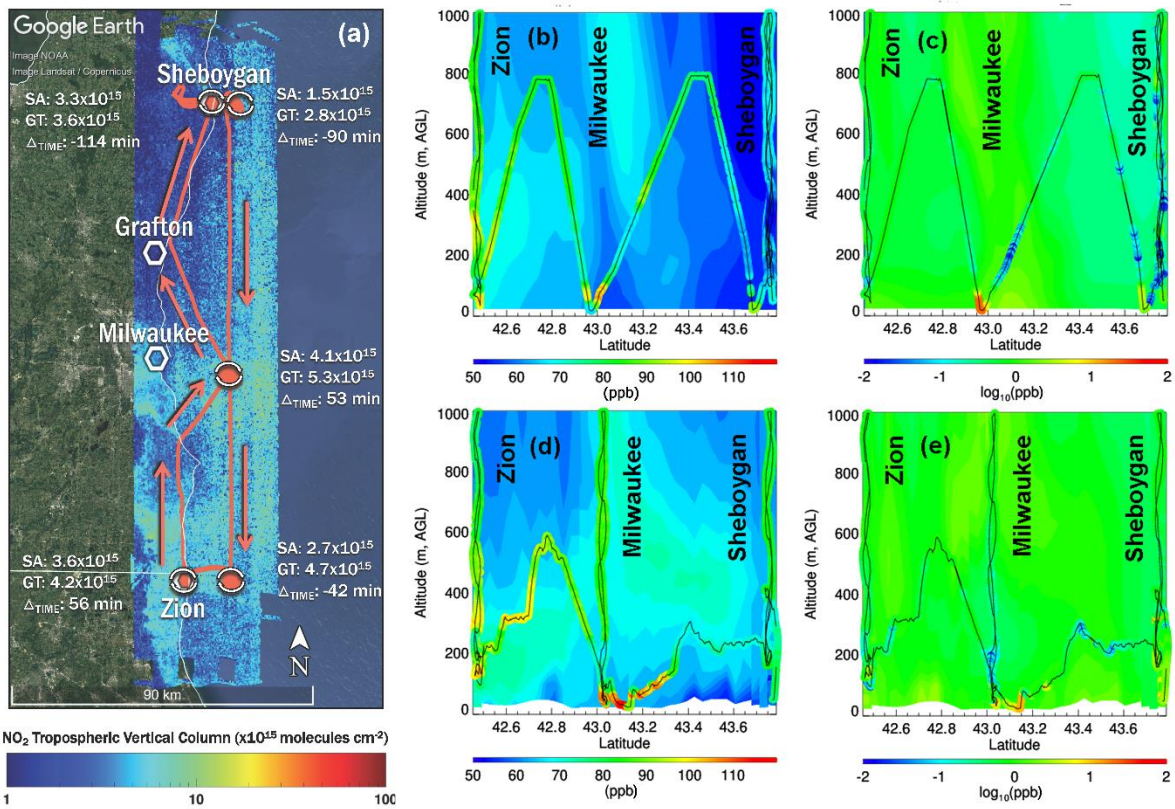

Figure 6. Aircraft mapping and profiling for 2 June. (a) NO_2 tropospheric vertical columns (molec cm^{-2}) collected by GeoTASO (GT) with the Scientific Aviation (SA) flight track overlaid (orange). White circles indicate the five locations where surface-to-3-km spirals were executed to collect vertical profiles. Coincident SA and GT columns are labeled (molec cm^{-2}) along with the difference in time in minutes (SA minus GT). North-to-south transect (southbound legs) observations of ozone (ppb, b) and NO_2 (log10 (ppb), c) from SA are overlaid on WRF-Chem modeled O_3 and NO_2. South-to-north transect (northbound legs) observations of O_3 (ppb, d) and NO_2 (log10 (ppb), e) from SA are overlaid on simulated O_3 and NO_2 mixing ratios from WRF-Chem.

Accepted for publication in *Bulletin of the American Meteorological Society*. DOI 10.1175/BAMS-D-20-0061.1.

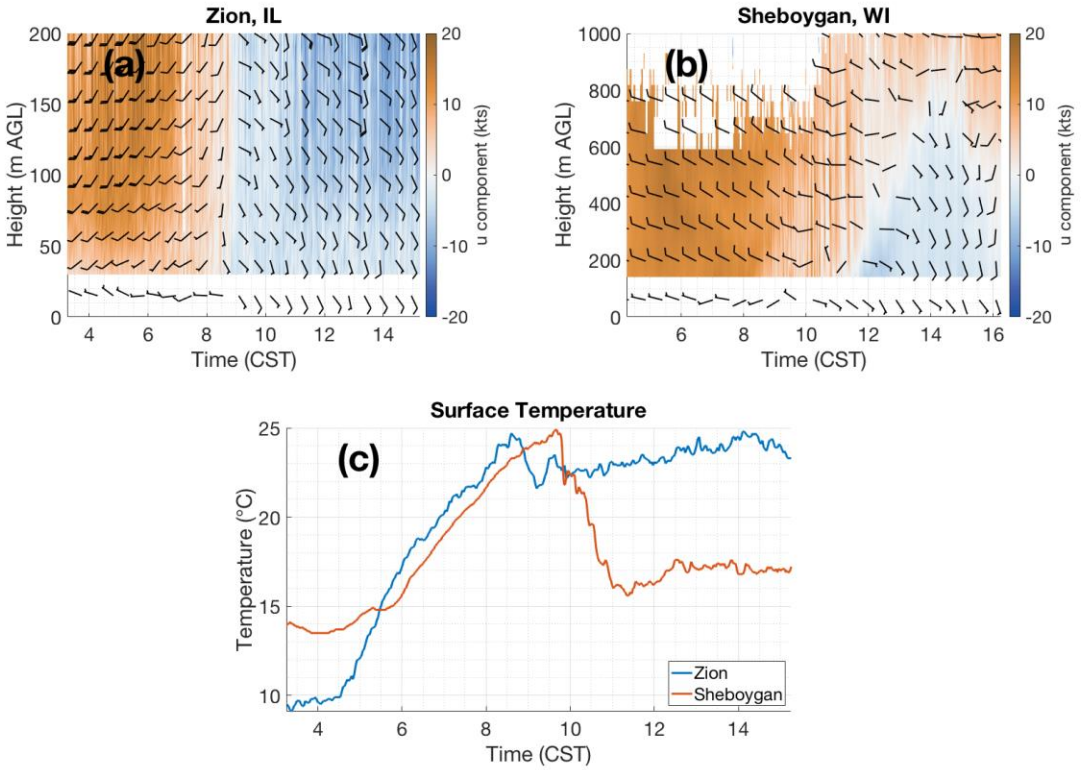

826

827 **Figure 7**. Winds (kts) observed by (a) sodar at Zion, Illinois and (b) Doppler lidar at the

828 Sheboygan site, and (c) surface air temperature (°C) during the 2 June 2017 lake breeze event.

829 Note the different vertical scale for the two wind cross sections. In wind cross sections, wind

830 barbs closest to the surface are from collocated 10-m wind; the 10-m are displaced upward to

831 enhance readability.

832

833

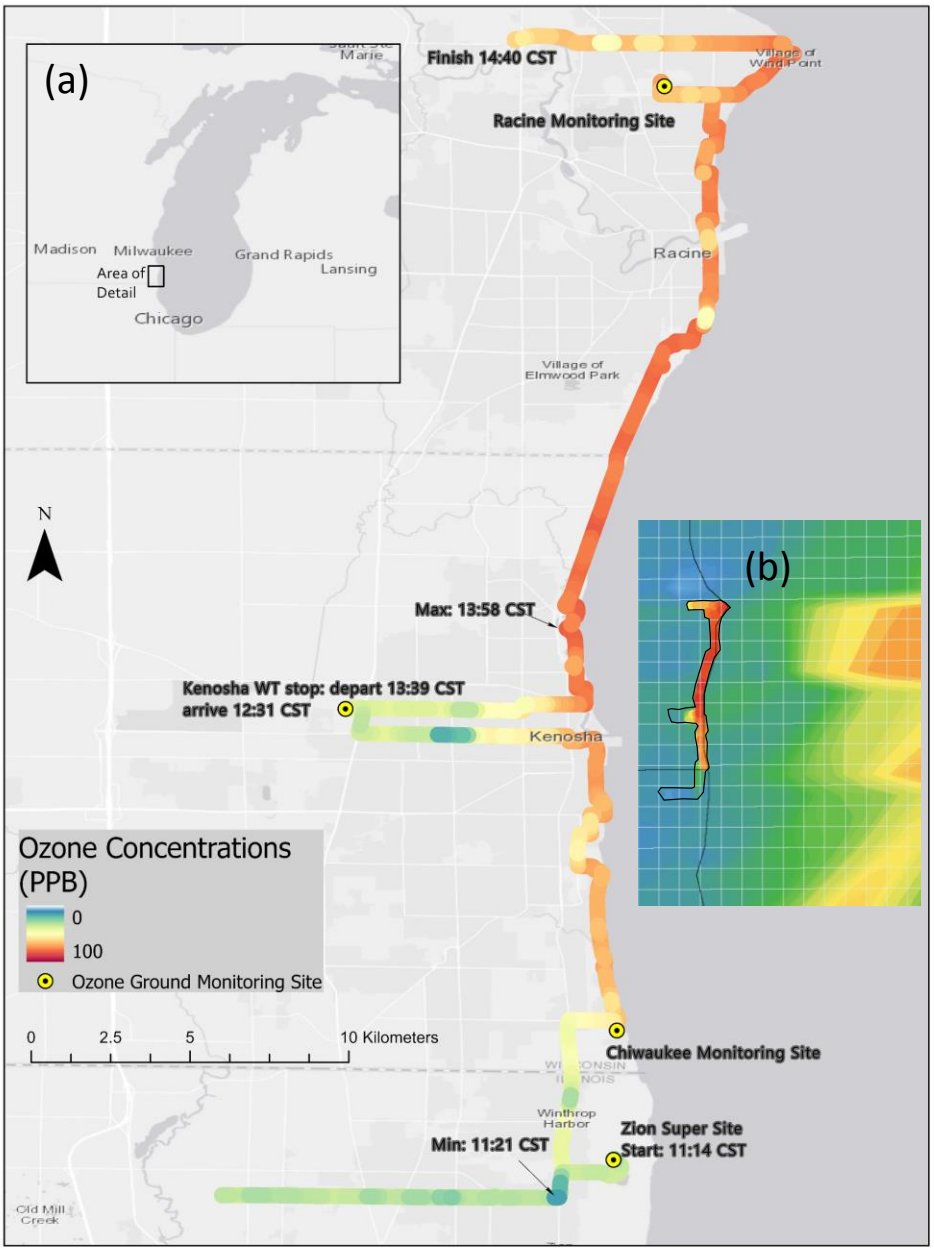

Figure 8. Mapping of intense ozone spatial gradients using GMAP. The GMAP vehicle trajectory on 12 June 2017 was from south-to-north, pausing for co-located measurements at Zion (1114 CST), Chiwaukee (1214 CST), Kenosha (1231-1339 CST), and Racine (1423 CST). Panel (a) shows the area of detail relative to Lake Michigan, while panel (b) shows the WRF-Chem simulation relative to the GMAP drive.